A Segmented Attenuation Correction for PET

Eddie Zhihua Xu, Nizar A. Mullani, K. Lance Gould, and Wallace L. Anderson

Electrical Engineering Department, University of Houston and Division of Cardiology, University of Texas Medical School, Houston, Texas

A segmented attenuation correction technique has been developed for positron emission tomography which computes attenuation correction factors automatically from transmission images for use in the final image reconstruction. The technique segments the transmission image into anatomic regions by thresholding the histogram of the attenuation values corresponding to different regions such as soft tissue and lungs. Average values of attenuation are derived from these regions and new attenuation correction factors are computed by forward projection of these regions into sinograms for correction of emission images. The technique has been tested with phantom studies and with clinical cardiac studies in patients for 30- and 10-min attenuation scan times. This method for attenuation correction was linearly correlated (slope = 0.937 and r^2 = 0.935) with the standard directly measured method, reducing noise in the final image, and reducing the attenuation scan time.

J Nucl Med 1991; 32:161–165

The accuracy of data recovery from positron emission tomography (PET) depends on the correction for attenuation of the emitted photons within the body (*1*). Failure to correct for attenuation in PET causes severe image artifacts the severity of which depends on several factors such as body size, shape, and heart orientation. An example of image artifacts due to omission of attenuation correction is shown in Figure 1 for myocardial perfusion imaging in a patient using nitrogen-13- (^{13}N) ammonia and the TOFPET I positron camera (*2*). Transaxial images of the heart were reconstructed with and without attenuation correction. At the mid-level of the heart, short-axis cross-sectional profiles from the lateral to the septal walls are shown below each transaxial image. Radiation emanating from the parts of the body near the center is reduced due to attenuation by body tissue. In the heart, the imaged tracer in the septal and inferior-posterior parts of the myocardium can be 30%–50% lower than the anterior portion due to attenuation. Lung activity is artificially enhanced due to lower attenuation for the radiation in the lungs.

Received Mar. 23, 1990; revision accepted June 8, 1990.

For reprints contact: Nizar A. Mullani, Div. of Cardiology, Univ. of Texas Medical School, 6431 Fannin St., Houston, TX 77225.

The amount of attenuation of cardiac activity depends greatly on the size of the patient's torso and the size of the breasts. To illustrate the problem, Figure 2 compares the relative myocardial perfusion with no attenuation correction for two different sized patients in order to demonstrate the quantitative effect of attenuation. The heart was divided into five sections; anterior, lateral, septal, inferior, and apical. The effects of attenuation were quantified on the tracer uptake in each section of the heart. Data from the images without attenuation correction were divided by data from images with attenuation correction. Myocardial perfusion in the image without attenuation correction is then expressed as a percentage of the corrected image for each section. A comparison of a 100-lb patient with a 200-lb patient shown in Figure 2, demonstrates the variability of data recovery from the posterior and inferior parts of the heart in the absence of attenuation correction.

There are two current methods for attenuation correction, i.e., the measured method and the geometrical method. The measured method derives the attenuation correction factors (ACF) from a transmission scan obtained with an external radiation source outside the patient. The geometrical method computes the ACF values from regions drawn or outlined from the attenuation image obtained from the transmission data. Computed values of ACF have less noise and therefore cause less noise in the emission images. However, drawing regions requires operator intervention and its accuracy is therefore operator dependent.

Automatic methods for feature extraction from transmission images (*3*) to find the boundaries of an object and compute ACF have been limited in clinical application due to difficulties in applying feature extraction methods to noisy images. Conventional edge-detection methods such as gradient and Laplacian (*4*) do not work well in noisy images and result in false edges of the boundary being detected. The noise can be reduced by smoothing the image before feature extraction, but smoothing blurs the boundaries and affects the corrected emission images.

Ganti et al. (*5*) have previously proposed a multi-resolution method to extract homogeneous regions by using a multi-resolution pyramid representation as a means of identifying the regions in the attenuation images. This technique was successful in detecting the

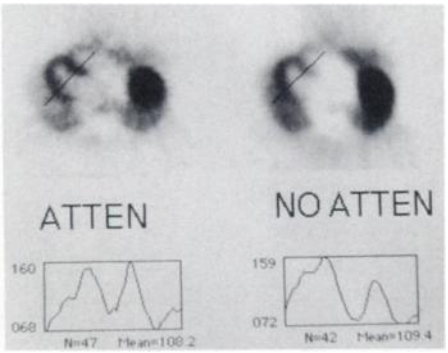

FIGURE 1
Transaxial images of myocardial perfusion obtained with nitrogen-13-ammonia and the TOFPET I positron camera. The image on the left is corrected for attenuation correction while the one on the right is not. Short-axis cross-sectional profiles of the heart drawn from the lateral to the septal regions are displayed below each image. Lack of attenuation correction enhances the lung activity and reduces the septal and inferior quantitation.

boundaries of an object but the computation time required was longer than the time required for acquiring a good attenuation scan for direct ACF measurement.

A new method which incorporates both measured and geometric techniques has been developed. It utilizes a priori knowledge that a transmission image of the torso comprises muscle, fat, blood, bone, lung, and patient couch. Attenuation coefficients for muscle, fat, blood, and bone are fairly similar and homogeneous for 511 keV radiation (*6*) while for the lungs the coefficient is approximately one-third of that for the tissue. Automatic region identification from transmission images is then based on the a priori knowledge that two regions, soft tissue and lungs, are easily identified by segmenting the attenuation coefficients into two values. We refer to this approach as the segmented attenuation correction (SAC) method. It has been tested in phantoms and clinical studies and is described below.

MATERIALS AND METHODS

Attenuation coefficients for soft tissue and bones for 511 keV gamma photons are 0.084 and 0.105 per cm, respectively (*6*). For a particular tissue such as muscle, the attenuation values are quite homogeneous in the body as demonstrate ' by X-ray computed tomography (CT). The higher energy (the 511 keV radiation combined with the low number of photons in the image makes it difficult to distinguish between muscle, bone, and fat with PET. Lungs, on the other hand, are significantly different in attenuation values (ranging from 0.02–0.04 per cm) and can be easily distinguished from soft tissue with PET.

Automatic Detection of Regions

A typical attenuation image obtained at the level of the thorax is shown in the top part of Figure 3. To the right of the image is a frequency histogram of the attenuation values. On the horizontal axis, attenuation values are normalized with respect to 255 and the vertical axis shows numbers of pixels. The histogram has three peaks which are attributed to the background, the lungs (and part of patient bed), and the soft tissue. Small regions of interest (ROIs) were visually drawn in the lungs and the heart muscle. Frequency histograms for these regions are displayed in the middle and lower images in Figure 3 for identification of the three peaks.

Applying the a priori information that the attenuation image consists of soft tissue (including bones), lungs (including patient couch), and background noise, the image can be segmented into three regions which are characterized by their attenuation coefficients. Two thresholds can be set for different attenuation values to identify soft tissue, lungs, and the patient couch. Tissue attenuation coefficients do not vary significantly from patient to patient and for a given PET system the measured coefficients are quite similar. We aver-

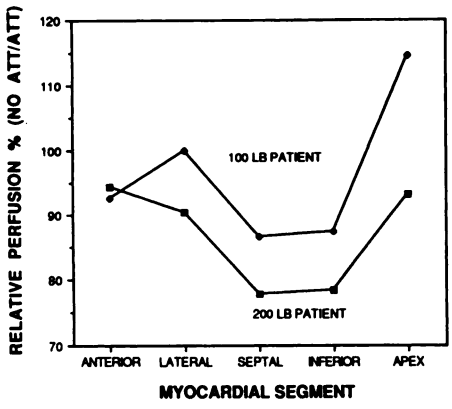

FIGURE 2
Relative myocardial perfusion is computed for five sections of the heart by dividing the no attenuation corrected data by the attenuation corrected data. There is large variability in relative perfusion from patient to patient as demonstrated with this example of 100-lb and 200-lb patients.

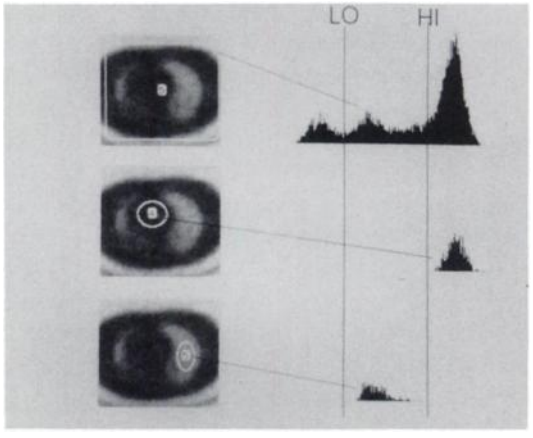

FIGURE 3
A typical attenuation image obtained with PET is shown together with its frequency histogram of the attenuation values to the right of the image. Three peaks in attenuation values are observed. Smaller regions drawn in the lungs and the heart identify the peaks in the middle and lower images.

aged attenuation density data from eight patients and determined that approximate values of 50 for the low-threshold and 130 for the high-threshold could identify the lungs and muscle regions.

The sizes of the segmented regions of the attenuation scans change as a function of the threshold values selected and therefore the attenuation lengths computed from the segmented attenuation images will also change. The change in attenuation lengths causes a change in the ACF, which can effect the accuracy of quantitation in the heart. An under-correction for attenuation results in lower recovery of activity from the center of the torso (reduced activity from the posterior part of the heart) while an over-correction causes an increased recovery of activity from the center of the heart (increased activity from the posterior part of the heart). A correct value of attenuation correction causes uniform recovery of activity from the center to the periphery of the torso.

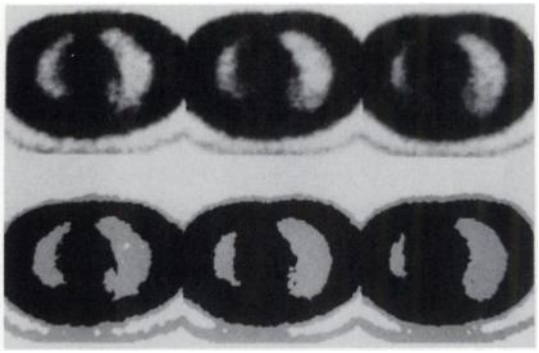

FIGURE 5
An example of segmentation of the regions is shown for three slices of a typical attenuation image collected with a 30-min attenuation scan at the level of the heart (top). The segmented images at the bottom were obtained with a high threshold of 136 and a low threshold of 50. Soft-tissue region is shown in black while lungs and patient couch are shown in gray.

Selection of Thresholds

The selection of the two thresholds for identifying soft tissue and lungs was carried out empirically in a two-step process. The first step was to set the thresholds in the valleys between the peaks shown in Figure 3 at approximate values of 50 and 130. The second step involved adjusting these thresholds to produce clinical PET quantitation comparable to that obtained with the measured method for attenuation correction. A selected number of normal clinical studies were corrected with the SAC method and compared visually with the original images for similar recovery of activity from different parts of the torso. Distribution of activity in different regions of the heart were compared for the two sets of images using the polar map quantitation software currently used in clinical nuclear cardiology (*7*). From the preliminary analysis of a few test cases, we determined that the quantitative recovery of activity from all the regions of the heart (whole heart quantitation) was quite sensitive to attenuation correction. Tracer uptake in the heart was quantified by polar map display normalized to the top two percent of activity in each image. Figure 4 shows the whole heart quantitation as a function of the high- and low-thresholds selected. Based on this data, we selected a threshold value of 136 for soft tissue and 50 for lungs. The low-threshold was set as high as possible in order to reduce the effect of background noise on region identification. An example of automatic edge-detection using the segmentation of the attenuation coefficients is shown in Figure 5. Three slices of PET attenuation images are shown on the top and their corresponding segmented images are shown below. The segment corresponding to the soft tissue is shown in black and the lung segment is shown in gray.

Computation of New Attenuation Correction Factors

Once the regions are identified, average values for the attenuation coefficients measured from the transmission scan are computed for each region. These values are then used to replace the measured values for each pixel in the image. The new values of attenuation for each pixel in the image are forward projected (the reverse of backprojection) onto sinograms, which are then used to correct the emission sinograms for attenuation. Computation of new attenuation sinograms was carried out on DEC VAX 11/780 computer and required 15 min of computation for each patient.

Evaluation of SAC Method with a Pie Phantom

An eight-sector pie phantom filled with different concentrations of radioactivity in each sector was imaged with the TOFPET I PET camera (*8*). The radionuclide concentrations for each sector were 1.0, 0.75, 0.625, 0.438, 0.25, 0.19, 0.063, and 0.0. Nine slices were collected simultaneously. Two attenuation scans were collected, one containing 15 million counts and the other 200 million counts for all nine slices. The 200 million counts is typical for attenuation scans performed for

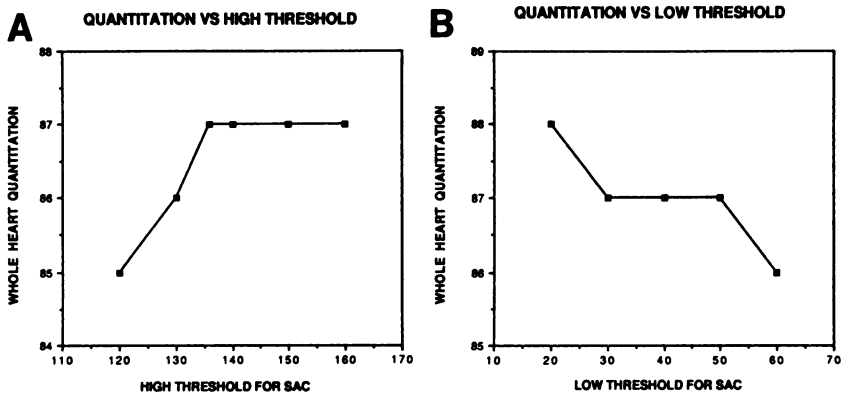

FIGURE 4
Selection of the two thresholds was carried out by examining the relationship between the two thresholds and polar map quantitative recovery for the whole heart. (A) Quantitation versus the high threshold for soft tissue. (B) Quantitation for the low threshold.

clinical cardiac or brain imaging. ACFs were computed using the measured method and the SAC method. Emission images were then corrected using the measured method and the SAC method. ROIs were drawn in each sector and the mean and standard deviations of each ROI were obtained.

Evaluation of SAC Method with Clinical Studies

Two sets of clinical studies were evaluated with the SAC method. The first protocol compared the measured attenuation correction based on a 30-min transmission data collection to the SAC method of attenuation correction in ten patients undergoing rest/dipyridamole myocardial imaging with the TOFPET I PET camera. In the second protocol, seven patients had an additional 10-min transmission scan to compare the SAC method based on a 10-min transmission scan to the standard measured method of attenuation correction based on a 30-min attenuation scan. Each patient had two emission scans (rest and dipyridamole) analyzed using the polar map method previously described (*7*). The heart was divided into five regions; anterior, lateral, inferior, septal, and apical. The uptake of a radionuclide in each region was quantified as an average percent of the maximum 2% of activity in the heart. For each patient study, 10 regions were evaluated for a total of 100 regions for the first protocol and 70 regions for the second protocol.

RESULTS

Pie Phantom Data

Transaxial images of the pie phantom were obtained with the measured attenuation correction and by using the SAC method. The image corrected for attenuation containing 15 million counts for all nine slices was quite noisy in appearance. The image corrected for attenuation based on an attenuation scan containing 200 million counts for all nine slices, or ~ 25 million counts for the slice displayed, showed an acceptable amount of noise. The image corrected with the SAC method derived from the 15 and the 200 million counts attenuation scans collected over 2 min and 30 min, respectively, showed better quality. The SAC method was able to reduce the noise in the 15-million count attenuation correction to almost the same level as the 200-million count image. Quantitative data from small ROIs drawn in each sector of the pie phantom are shown in Table 1. The level of noise in the image is indicated by the standard deviation of the data. The SAC method was able to significantly reduce the scan time. A typical 15-million count attenuation acquisition takes about 2 min compared to 30 min for 200-million count attentuation.

Evaluation of Clinical Images by Quantitative Polar Map Analysis

Clinical images were reconstructed with the measured attenuation correction method and the SAC method. An example of the image quality obtained with the two protocols is shown in Figure 6 for a patient with anterior-septal perfusion deficit imaged with rubidium-82 (^{82}Rb). Examples of the 30-min and 10-min attenuation scans are shown on the left. Emission images corrected with the measured attenuation correction are shown in the center with emission images corrected by the SAC method on the right.

TABLE 1
Recovered Pie Phantom Quantitation Corrected for Attenuation with 15 and 200 Million Measured Counts and with the SAC Method*

Pie sector	Measured [15 M]		Measured [200 M]		SAC [15 M]		SAC [200 M]	
0	100	(5.0)	100	(1.1)	100	(1.9)	100	(1.4)
1	93.0	(7.3)	77.3	(1.9)	80.3	(2.3)	79.4	(2.8)
2	71.6	(4.9)	66.2	(2.5)	66.0	(1.8)	65.5	(1.3)
3	57.6	(6.8)	50.7	(4.6)	49.0	(1.6)	48.2	(1.7)
4	29.2	(11.3)	28.4	(2.5)	29.5	(2.0)	29.0	(2.5)
5	22.5	(15.1)	22.2	(4.9)	22.5	(4.4)	21.8	(3.8)
6	8.4	(50.1)	8.2	(17.5)	7.9	(6.5)	7.8	(6.9)
7	3.0	(93.2)	2.6	(22.4)	1.9	(35.7)	1.8	(39.1)

* Each sector of the pie phantom was filled with varying concentrations of radioactivity. The recovered data is normalized to 100% for the highest activity. Percent s.d. for each sector is shown in parentheses.

The two sets of clinical images were evaluated using the automated polar map analysis software. Quantitative data for the five regions of the heart corrected with 30 min measured attenuation correction were compared to the data obtained with the SAC method correction derived from the 30-min measured attenuation image. A linear fit was found between the quantitative values obtained with the two methods. A slope of 0.975 and a r^2 value of 0.916 were found for the 30-min protocol. A similar linear fit between the 30-min measured attenuation correction quantitation and the SAC

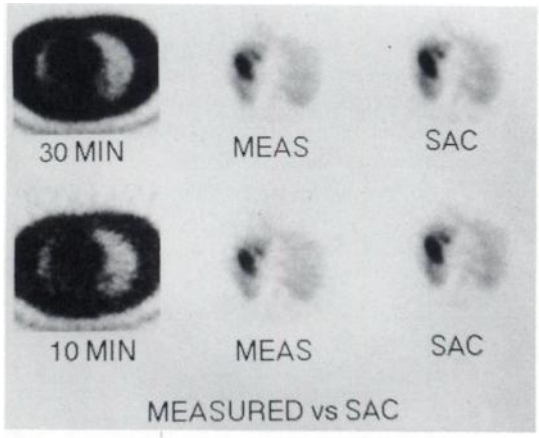

FIGURE 6
An example of a clinical patient study reconstructed with 10- and 30-min attenuation scans obtained in a patient with anterior septal perfusion defect. Attenuation images are on the left and emission images corrected with measured attenuation correction are in the middle. The corresponding SAC images show that the noise level is reduced and no artifacts are introduced with this method.

method quantitation derived from the separate 10-min measured attenuation image was found. The slope of the line was measured at 0.966 and the r^2 value was 0.93. The combined data for the two protocols (17 patients, 170 regions) show a strong linear correlation with a slope of 0.937 and a r^2 value of 0.935 for the measured attenuation correction against the SAC method as shown in Figure 7.

DISCUSSION

We have shown with phantom and clinical data that the SAC method for attenuation correction is comparable in quantitation to the measured method for attenuation correction for PET. We have also shown that the 10-min SAC method results in comparable quantitation to the 30-min measured method. Reducing the attenuation scan time for application of PET is important for efficient clinical operation and for improving image quality. This approach can reduce the total scan time for rest/stress ^{82}Rb imaging of the heart by 20 min (from 60 min to 40 min). The shorter scan time has other implications for wider clinical application of PET. It can improve throughput or the number of studies per day thereby making PET more economical. Shorter scan times make it more feasible to use PET in acute myocardial infarction protocols for ruling out myocardial infarction and for monitoring thrombolysis protocols where prolonged imaging protocols are not appropriate.

Caution should be exercised when implementing this technique with other organs and with other PET cameras. The two thresholds used in this work were empirically derived from the attenuation images and selected to match the quantitation obtained with measured attenuation corrections. These thresholds may be different for different PET systems. A shift in the attenuation histogram, which is attributed primarily to a high number of random coincidences in the attenuation data, was observed at very high count rates. Therefore, the optimal thresholds for SAC for each PET system may have to be determined individually. We also used the average attenuation coefficient measured with the transmission scan in the segmented images for the calculation of ACF to simplify the SAC method even further. The average attenuation coefficients could be replaced by theoretical attenuation coefficient values for theoretically better corrections, independent of the effects of randoms, scatter, and backscattered radioactivity in the object. It is possible to use the SAC method in the presence of radioactivity in the object. The attenuation scan could be obtained between rest and dipyridamole scans (during the infusion of dipyridamole) thereby shortening the total procedure time considerably.

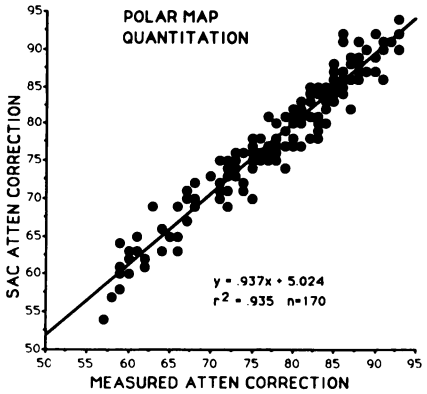

FIGURE 7
Combined data for the two protocols (17 patients, 170 regions) are compared for the measured versus the SAC method. All SAC patient quantitation is compared to all 30 min measured quantitation.

CONCLUSIONS

The SAC method for attenuation correction of PET scans shortens the attenuation scan time and maintains the same or better quantitation in comparison with directly measured attenuation corrections. Further testing of this promising approach will be necessary before routine clinical applications.

ACKNOWLEDGMENTS

The authors wish to thank the following: T. Lee and M. Chang for their help in the data transfer and analysis; M. Haynie, M. Hess, and D. Patel for their assistance in acquiring the PET data; and R. Edens for editorial assistance. This work was carried out as joint collaborative research with the Clayton Foundation for Research and was partially funded by the Department of Energy contract DE-FG05-84ER60210, and NIH grants R01-H1-26862 and R01-HL-268551.

REFERENCES

1. Huang SC, Hoffman EJ, Phelps ME, Kuhl DE. Quantitation in positron emission computed tomography. 1. Effects of inaccurate attenuation correction. *J Comput Assist Tomogr* 1979;3:804–814.
2. Gould KL, Mullani N. Routine clinical positron emission tomography for diagnostic cardiac imaging—a review. *Herz* 1987;12:13–21.
3. Huang SC, Carson RE, Phelps ME, Hoffman EJ, Schelbert HR, Kuhl DE. A boundary method for attenuation correction in positron computed tomography. *J Nucl Med* 1981;22:627–637.
4. Rosenfeld A, Kak AC. *Digital picture processing*, 2nd edition, Vol. 2. Orlando, Florida: Academic Press; 1982.
5. Ganti G, Ranganath MV, Mullani NA, Gould KL. A multi resolution method for attenuation correction in positron emission tomography. *J Nucl Med* 1989;30:880.
6. Sorenson JA, Phelps ME. *Physics in nuclear medicine*, 2nd edition. Orlando, Florida: Grune & Stratton; 1987.
7. Hicks K, Ganti G, Mullani NA, Gould KL. Automated quantitation of three-dimensional cardiac positron emission tomography for routine clinical use. *J Nucl Med.* 1989;30:1787–1797.
8. Mullani NA, Gaeta J, Yerian K, et al. Dynamic imaging with high resolution time-of-flight PET camera—TOFPET I. *IEEE Trans Nucl Sci* 1984;NS-31: 609–613.